STATIC AND DYNAMIC COMPRESSIBILITY OF DEEP UNDERGROUND CAVERNS

P. Bérest, J. Bergues, B. Brouard
Laboratoire de Mécanique des Solides
Centre commun X, Mines, Ponts, URA 317 CNRS
Ecole Polytechnique
91128 Palaiseau France

October 14, 1999

Abstract

Compressibility of deep fluids-filled cavern is discussed. Compressibility is measured both through statical and dynamical tests. Statical compressibility is influenced by cavern shape and cavern fluids nature. This parameter plays an important role for such applications as the determination of stored hydrocarbons volume, of volume lost during a blow-out, and of pressure build-up rate in a closed cavern. Dynamical compressibility is measured through the periods of waves triggered by pressure changes. Both tube waves and longer period waves associated to the existence of an interface between a liquid and a gas can be observed. They can provide additional information, for instance the existence of trapped gas in the well-head.

Introduction

In this paper we consider deep caverns (from 300 m to 2000 m and more) that are connected to ground level through a cased and cemented well, which allows injection or withdrawal of fluids into or from the cavern.

These caverns are, in general, leached out from salt formations. The purpose of these caverns is to provide chemical plants with brine or, more commonly, to provide storage of large quantities of hydrocarbons. The volumes of such caverns range from 5,000 m^3 to 1,000,000 m^3.

The mechanical behavior of such caverns is relatively complex, as rock salt rheology exhibits some unusual features. Many laboratory works have been devoted to it, but the subject hardly seems to be exhausted [1–4].

The general outline for the mechanical behavior of caverns is similar to that for a rock sample, but a clear understanding may require additional comments.

One can distinguish among the following:

- Long-term steady-state creep is reached when the cavern fluid pressure is kept constant for months or years. A typical value of relative cavern volume change rate due to steady-state creep for a 1000-m deep cavern submitted to *halmostatic* pressure (or the pressure of a cavern when the well is filled with saturated brine up to ground level, where it is opened to atmosphere — i.e., 12 MPa) is $3\ 10^{-4}$ per year. This value should be multiplied by 100 when the cavern is 2000 m deep (The *halmostatic* pressure equals 24 MPa.), because of the increases in both lithostatic pressure and temperature. In any case, these features are subject to large variations when different sites and cavern shapes are considered.

- Transient creep is triggered by any significant and rapid cavern pressure change. Its effect on the relative volume change rate can be one or two orders of magnitude larger than the steady-state value at the same average pressure level, but it is significant for only a few weeks (see, for instance, Hugout [5]). The transient creep effects in a cavern, even if very significant, are difficult to assess, for they are interlocked with the effects of the additional salt dissolution or brine recrystallization which, as transient creep, follow any cavern pressure change (Ehgartner and Linn [6]). The "true" transient creep must be distinguished from the effect of steady-state creep changes that lead to a transient redistribution of the non-uniform stress field around the cavern, slowly moving from its initial to final distribution. This transient evolution can be several years long.

- Elastic behavior of the cavern, or cavern shape and volume changes, immediately follow any cavern pressure change. (As will be seen later, "immediately" requires definition.)

This last aspect has not yet been given much attention in the literature when compared to creep, which is of primary importance

for cavern structural stability and life-long duration. Nevertheless, the elastic behavior of a cavern — more precisely, cavern compressibility — plays a very significant role in various phenomena, including mechanical-integrity test design (see Bérest *et al.* [7]), pressure build-up rate in a closed cavern and blow-out scenarios (discussed later), among others. Useful information on cavern volume, the existence of trapped gas pockets and evaluation of the amount of hydrocarbon stored can be inferred from such measurement.

As for the mechanical behavior of any elastic body, cavern compressibility is apparent both through static and dynamic tests (i.e., involving waves triggered by a rapid change of pressure). These two aspects will be discussed successively.

Furthermore, it must be kept in mind that changes in cavern volume or shape cannot be directly observed; they are measured through experiments that involve flow and/or pressure measurements at the well-head. Brine (or, in general, stored fluids) properties, and mass transfer from salt mass to brine influence the measurements results and must be taken into account, together with the mechanical properties of salt, for a thorough interpretation of the tests.

1 Static Behavior

1.1 Cavern Compressibility and the Compressibility Factor

When a certain amount of liquid, ΔV_{inj}, is injected in a closed cavern, the well-head pressure increases by ΔP which is also, at first approximation (see paragraph 1.5.1) the cavern pressure increase ΔP_c. The relation between the two quantities is, in general, fairly linear during a rapid test. The slope of the curve (brine pressure versus injected brine) is called the *cavern compressibility* (in m^3/MPa or bbls/psi):

$$\Delta V_{inj} = \beta V \ \Delta P$$

As a matter of fact, compressibility, βV, can be expressed as the product of the cavern volume, V (in m^3), and a *compressibility factor*, β (in vol/vol/MPa, or vol/vol/psi). The compressibility factor, β, is a constant — at least for caverns of similar shapes located in the same site, filled with the same fluid and tested during a relatively short period (one hour); in other words, β is not dependent upon the *size* of the cavern.

1.2 The Compressibility Factor

We first consider the case of a brine-filled cavern. Let M be the cavern brine mass: $M = \rho_b V$, where ρ_b is the brine density, and V is the cavern volume.

When the cavern pressure rapidly increases by ΔP_c (by "rapidly" we mean that neither salt creep nor brine dissolution are afforded enough time to play a significant role), the following occurs:

1. The brine density increases by $\rho_b \beta_b^{ad} \Delta P_c$, where β_b^{ad} is the brine adiabatic compressibility factor. It does not depend upon cavern shape or cavern volume.
2. The cavern volume increases by $\Delta V = \beta_c \Delta P_c V$, where β_c is the cavern compressibility factor, which depends upon rock-mass elastic properties and cavern shape (but *not* upon cavern volume).

Then, if an additional mass of saturated brine, $m = \rho_b \Delta V_{inj}$, is forced into a closed cavern, its pressure will increase by

$$M + m = (\rho_b + \Delta\rho_b)(V + \Delta V)$$

or

$$\beta V \Delta P = \Delta V_{inj} \qquad ; \qquad \beta \approx \beta_b + \beta_c$$

The compressibility factor, β, is the sum of the brine compressibility factor, β_b, and the cavern compressibility factor, β_c.

1.3 The Cavern Compressibility Factor

The cavern compressibility factor, β_c, obviously depends upon both rock-salt elastic properties and cavern shape.

1.3.1 Theoretical Analysis

For simple cavern shapes, some analytical calculations can be made. If E is the Young's modulus of the salt and ν is its Poisson's ratio, we get the following:

cavity shape	sphere	infinite cylinder	real-world
β_c	$\frac{3\ (1+\nu)}{2E}$	$\frac{2(1+\nu)}{E}$	$f(\nu)\ .\ \frac{(1+\nu)}{E}$

where $f = f(\nu)$ is a *shape factor* that depends on the cavern's shape and, to a smaller extent, on the Poisson's ratio of the rock; and f is always greater than 3/2, which corresponds to the spherical case, which is the less compressible shape of a cavern. The shape factor can be computed for any cavern shape; it is much larger than 2 in the case of a flat cavern.

1.3.2 Field Data

From compressibility factor data, Boucly [8] infers that $\beta_c = 1.3\ 10^{-4}$ /MPa ($9.0\ 10^{-7}$ /psi), which is consistent, for instance, with the following estimates:

$$\nu = 0.3 \qquad E = 17,000 \text{ MPa} \qquad f = 1.7$$

This shape-factor value corresponds to caverns from the Tersanne and Etrez sites whose shapes are intermediate between cylindrical and spherical. The elastic properties of rock salt can vary from one site to another.

1.4 The Fluid Compressibility Factor

1.4.1 Brine

The theoretical adiabatic brine-compressibility factor is related to the sound of speed through the relation $\rho_b \beta_b^{ad} c_b^2 = 1$, where $\rho_b = 1200$ kg/m^3, $c_b = 1800$ m/s; thus , $\beta_b^{ad} \approx 2.57\ 10^{-4}$ /MPa. This figure suits rapid (adiabatic) evolutions, β_b^{ad} is not different, from a practical point of view, from the brine isothermal compressibility factor, but it is a little too small when relatively slow pressure changes (several hours or days long) are considered, because the brine saturation concentration is modified by pressure change. Pressure build-up triggers additional cavern leaching, (as noted, for instance, by Ehgartner and Linn [6]) and increases the cavern volume, resulting in a slightly higher effective brine compressibility factor. When creep is neglected the following approximation holds:

$$\Delta V_{inj} = \beta^{sat} V \Delta P \approx \left(\beta_c + 1.06\ \beta_b^{ad}\right) V \Delta P$$

This additional compressibility is not immediately effective, because salt dissolved at a cavern wall must be transported through convection and diffusion until chemical equilibrium in the whole brine body is restored. Kinetics are difficult to assess and impossible to measure in situ, as dissolution effects and transient creep effects are interlocked.
As a conclusion, a reasonable value for the in-situ brine compressibility factor seems to be $\beta_b = 2.7\ 10^{-4}$ /MPa ($1.9\ 10^{-6}$ /psi), Boucly [8] or Crotogino [9] but it must be kept in mind that this value can be influenced by test duration.

1.4.2 Hydrocarbons

Hydrocarbons are much more compressible than brine or water. Their compressibility factors are influenced by pressure and temperature. A typical value for pure propane at 25 ^{o}C and 7 MPa is $\beta_{prop} \approx 2.9\ 10^{-3}$ /MPa; it is slightly higher (up to $4.5\ 10^{-3}$ /MPa) for industrial propane.

1.4.3 Nitrogen and Other Gases

As long as only slow (less than one hour for a gas volume of a few cubic meters) evolutions are considered, gas evolutions can be considered to be isothermal; for an ideal gas (which nitrogen is, for the most part), the compressibility factor is simply the inverse of the (absolute) pressure, P:

$$\beta_{gas}^{isot} = 1/P$$

This means that the compressibility factor of a gas pocket trapped at the top of a brine-filled cavern (where the pressure is, for instance, $P_c = 12$ MPa at 1000 meters), will be

$$\beta_{gas}^{isot} \approx 8.3\ 10^{-2} \text{ /MPa} = (1/12) \text{ /MPa}$$

1.4.4 The Case of Several Fluids in a Cavern

• **Theoretical Aspects**

In a storage cavern, the cavity contains brine *and* another fluid (such as propane or oil). In this case, the global fluid-compressibility factor will be a certain average of the compressibility factors of the different fluids: β_b (for brine) and β_h (for hydrocarbon). Let x be the cavern volume fraction that is occupied by the other fluid [i.e., if V is the cavern volume, the hydrocarbon volume is xV and the brine volume is $(1-x)V$]. Then, the global compressibility factor β will be

$$\beta = \beta_c + (1-x)\beta_b + x\beta_h$$

This will vary, to a large extent, with respect to the hydrocarbon volume fraction. Consider, for instance, the case of propane storage. If we take

$$\begin{cases} \beta_c = 1.3\ 10^{-4} \text{ /MPa} \\ \beta_b = 2.7\ 10^{-4} \text{ /MPa} \quad \Rightarrow\ \beta = 4\ 10^{-4} + 42.3\ 10^{-4}\ x \text{ (/MPa)} \\ \beta_h = \beta_{prop} = 4.5\ 10^{-3} \text{ /MPa} \end{cases}$$

the compressibility factor varies from $\beta = 4\ 10^{-4}$ /MPa (no propane in the cavern) to $\beta = 38\ 10^{-4}$ /MPa (propane fills 80% of the cavern).

• **Example** — The SPR1 cavern in the Carresse site (in south-western France) is used by the SNEA(P) (ELF) company to store propane. The casing shoe depth is 348 meters below ground level; the cavern bottom depth is 381.5 meters. This cavern volume is 13,000 m^3 (as measured in 1992). We have performed compressibility factor measurements at three different periods (see Figure 1). During these three tests, the cavern compressibility (βV) was measured during a brine injection; the pressure measurement resolution was 500 Pa. This allows the propane volume in the cavern to be back-calculated . The computed propane volumes were compared with the operator's data obtained through surface flow-meters. The agreement with the above stated formula is satisfactory if not perfect. The reason may be that a definite testing protocol was not yet clearly set during the first tests.

1.4.5 The Case of a Gas Pocket in a Cavern

If a gas pocket is trapped in a cavern, the compressibility factor drastically increases, even if the pocket volume is small.

The SPR3 cavern of the SNEA(P) Carresse site is deeper than SPR1; the casing-shoe depth is 692 meters below ground level, and the cavern bottom depth is 711 meters. The cavern volume is $V \approx 4600$ m^3. A 1995 sonar survey performed a few months before the test confirmed that this cavern exhibits a non-convex shape (Figure 2). The compressibility factor observed during the test was $\beta \approx 11\ 10^{-4}$ /MPa, which appears abnormally high for a brine-filled cavern (pressure resolution was 500 Pa). It soon

appeared that this high figure could be explained by the presence of gas coming from the salt formation or from the brine used for cavern leaching, which was trapped in gas pockets under the bell-shaped parts of the cavern. These pockets are clearly visible on the left and top of the cavern shown on Figure 2. The gas pressure at cavern depth is $P_c = 8.3$ MPa, which means that its isothermal compressibility factor is $\beta_{gas}^{isot} = 0.12$ /MPa. The volume of the gas pocket can be back-calculated: it is approximately 25 m^3, or $x = 0.5\%$ of the cavern volume.

1.5 Phenomena Influencing the Measurement of Cavern Compressibility

Several phenomena can affect cavern compressibility measurements. For instance, brine in a cavern very slowly reaches thermal equilibrium with the rock mass (Bérest and Brouard, [10]), resulting in long term continuous thermal expansion. In most cases this effect is too slow to seriously affect a compressibility test. The same can be said of brine seepage through the rock mass, which is insignificant in this case. Transient creep, triggered by pressure variations, can be of some concern especially when the test is carrried out through brine withdrawal, as pointed out by Clerc-Renaud and Dubois [11]. But the main concern is raised by the density of the injected fluid. Assume that the injected brine is not fully saturated (for instance $\rho_b = 1180$ kg/m^3 instead of $\rho_b = 1200$ kg/m^3); then when a volume of unsaturated brine equal to ΔV_{inj} is injected in the central tube, the injected brine/saturated brine interface decreases by $h_i = \Delta V_{inj}/S$, S is the central tube cross-section, and the tube pressure change is different from the annular space pressure change, $\Delta P_{tub} = \Delta P_{ann} + \delta\rho g h_i$. If cavern compressibility is assessed through central tubing pressure measurements, the relative error made will be $g\beta V\,\delta\rho g/S$, which can be significant in the case of large caverns.
A similar effect can be reached if brine is so rapidly injected that thermal equilibrium with the rock mass surrounding the cavern is not reached during the test.

1.6 APPLICATIONS

Volume of Fluid Lost During a Blow-Out

During special operations in oil- or gas-filled caverns, eruptions can result from failure of the sealing-off equipment. From the perspective of risk analysis, it is important to evaluate the volume of fluids that would be released from the cavern upon total decompression.

If ρ_h is the density of a stored liquid hydrocarbon and ρ_b the brine density, and if the brine at the well-head is submitted to atmospheric pressure, then the hydrocarbon pressure at the well-head in the annular space is a linear function of the interface depth H_i:

$$P_{ann} = (\rho_b - \rho_h) g H_i$$

After failure of the well-head (see Figure 3), hydrocarbon pressure will drop to zero, and the brine level in the central tube will fall to a depth, η, such that the weight of the two fluid columns balance:

$$\rho_b(H_i - \eta) = \rho_h H_i$$

The pressure drop is $\rho_b g\eta$, and the percentage volume of fluid expelled from the cavern is mainly due to fluid decompression in the cavern:

$$V_{exp}/V = \left[\beta + x\left(\beta_h - \beta_b^{ad}\right)\right]\,(\rho_b - \rho_h) g H_i$$

where β is the average cavern compressibility factor and $\beta = \beta_c + \beta_b^{ad}$.

• For oil-filled storage ($x \approx 1$) in a 1000-meter deep cavern, the relative volume of expelled oil following well-head failure would be $2.7\ 10^{-3}$ (or 1,350 m^3 for an oil-filled 500,000 m^3 cavern). For propane storage in a 600-meter deep cavern, the relative volume of propane expelled would be $1.5\ 10^{-2}$ (or 750 m^3 from a propane-filled 50,000 m^3 cavern).

2 Dynamic Behavior

2.1 Introduction

In the previous section, we have seen that the fluid(s) contained in an underground cavern and access well, in addition to the cavern and the casing or strings, are elastic bodies. This means that when the fluid(s), the cavern or the well are affected by small changes in pressure or shape, these bodies vibrate according to their mechanical properties, sizes, shapes, and their mechanical interactions. These vibrations constitute a source of information that is rarely used, even when the cost of this information is minimal. All that is needed is to record the development of the fluid pressure at the well head. See Holzhausen and Gooch [12], Bérest [13], Hsu [14], Bérest *et al.* [15].

2.2 Tubing Waves

The first type of wave observed in salt caverns is a well wave, whose period is of the order of one to few seconds. When a rapid change in pressure and/or fluid flow rate takes place in a fluid-filled tube (for instance, when a valve is suddenly closed or opened), this change generates an acoustic wave that travels in the fluid along the well. If the tube were perfectly stiff, the wave celerity would be given by the simple formula

$$\beta_f^{ad}\rho_f c_f^2 = 1$$

where c_f is the acoustic wave celerity in the fluid. With standard temperature and pressure, typical values of the wave celerity are: $c_w = 1500$ m/s for soft water, $c_a = 340$ m/s for air, and $c_b = 1800$ m/s for saturated brine. In fact , the steel tube is also

a compressible body; and the global well compressibility factor, $\beta = \beta_t + \beta_f^{ad}$, is larger than β_f^{ad}, resulting in a speed of sound, c, in the well that is smaller than the fluid wave speed:

$$1/c^2 = 1/c_f^2 + \rho_f \beta_t$$

A typical value for water or brine in a tube will be $c = 1000$ m/s.

In this example, if the tube cross-section were $S = 250$ cm^2 (7"$^{5/8}$ in diameter) and the brine flow rate before closing the valve were $Q = 90$ m^3/h, the fluid speed would be $u = Q/S = 1$ m/s; the pressure increase behind the travelling down wave due to the sudden valve closure would be $\Delta P = \rho_f c u$ — or, in our case if fluid is brine, $\Delta P = 1.2$ MPa (205 psi). Such a phenomenon is called a "water-hammer"; the rapid pressure change shakes and rattles the tube in the well.

The tube shoe opens in so large a cavity (when compared to the very small volume of brine displaced by the wave itself) that, when the wave reaches the tube end, it is not able to modify the pressure in the cavity by any noticeable amount. Then a second wave, traveling upward and transporting a negative pressure change ($-\Delta P = -\rho_b c u$) is generated such that the pressure change, which had been generated by the primary downward wave, vanishes to zero below the upward wave. This wave reaches the well head and in its turn generates a downward wave. After a short time, theses waves combine to form a simple stationary wave; pressure changes or fluid-flow rate variations have the same phase along the entire tube. Pressure is constant at bottom, as noted above. Flow vanishes to zero at the top if the well head is closed, leading to a so-called "quarter-wave" vibration whose period is $cT = 4H$, H being the tube length. Two examples are given below.

• The first test (Figure 4) was performed in July 1995 on the Carresse SPR3 cavern. The cavern was filled with brine; its volume, as estimated by sonar, was 4600 m^3; and the cavern top was 692 meters deep. The observed vibrations were triggered by venting of the cavern, during which the well-head pressure suddenly dropped from 0.4 MPa to zero. The oscillation period was $T = 2.5$ seconds (Data acquisition frequency was 20 Hz, as in all tests described below, except for the 1982 Etrez 53 test), which means that $c = 4H/T = 4 * 692/2.5 \approx 1100$ m/s.

• The second test (Figure 5) was performed in February 1995 on the Etrez 53 cavern, as part of the full test program described by Bérest *et al.* [7]. The cavern volume was $V \approx 7500$ m^3; the 930 m-long central tube was filled with brine; a 140-meter high column of nitrogen was lowered into the annular space. In Figure 5, long period (20 seconds) oscillations are clearly observed; they are similar to the waves described in the next paragraph. Half-waves –for gas displacements vanish both at the well head and at the gas-brine interface– in the nitrogen column ($c = 345$ m/s, $h = 140$ m) are clearly visible for the instance between $t = 60$ s and $t = 70$ s; their periods are $T \approx 0.81$ s or $T = 2h/c$. Quarter-waves in the central brine-filled tube are also clearly visible (for example, between $t = 90$ s and $t = 150$ s; their period is approximately 2.6 s).

2.3 The Helmholtz Resonator

In the last paragraph, we considered waves generated by small displacements of the fluid contained in the tube and traveling through the well. An oscillatory phenomenon of another kind intervenes when the well-head is not closed; then large volumes of fluid can be exchanged between the well and the cavity itself, whose pressure now will not be considered as constant. The interface between the liquid and the air, whose seat will be in the well head or inside a container above the well-head (Figure 6), will experience movements of long period (one to several minutes).

2.3.1 Well Opened into a Large Container

Consider, first, a simple example consisting of a cavern and a well filled with brine and opened to the atmosphere in a container whose cross-section (Σ) can be much larger than the cross-section of the tube (S) — see Figure 6.

As seen before, both brine in the cavern and the cavern itself behave as springs, in the sense that both are compressible: a $\dot{P_c}$ pressure-variation rate in the cavern leads to a brine outflow rate through the cavern top, Q, such that:

$$(\beta_c + \beta_b^{ad}) V \dot{P_c} + Q = 0$$

where V is the cavern volume, β_c and β_b^{ad} are the cavern and brine adiabatic compressibility factors, respectively. The "dynamic" compressibility factor ($\beta = \beta_c + \beta_b^{ad}$) is slightly smaller than its static counterpart, but $\beta = 4\ 10^{-4}$ /MPa still appears a reasonable value.

The "stiffness" of a brine-filled (or "lower-spring") cavern (i.e., the ratio between brine flow and the pressure build-up rate), is the inverse of the cavern compressibility:

$$\Delta P/\Delta V_{inj} = 1/[(\beta_c + \beta_b^{ad})V]$$

For a 100,000 m^3 cavern, this ratio is $2.5\ 10^{-2}$ MPa/m^3; in other words, it is necessary to force a 40-m^3 volume of brine into the cavern to increase its pressure by 1 MPa.

The volume of brine contained in the central tube will appear, by comparison, as an extremely stiff body. The brine-plus-steel-tube compressibility factor may be not very different from the brine-plus-cavern compressibility factor, but the tube volume is smaller by 3 or 4 orders of magnitude than the cavern volume, resulting in much larger global stiffness ($1/\beta V$). As a whole, the brine in the tube can be considered as a rigid body (In fact,

tube waves due to brine compressibility in the tube, which had been described above, do exist, but they do not interfere, due to their much shorter period).

The brine in the container at ground level also behaves as a "spring" in the following sense: if a brine flow, Q (in m^3 per second), is expelled from the cavern, it will result in a Q/Σ uprise of the air/brine interface at the well head which, in turn, determines a pressure build-up at the well head:

$$\dot{P}_{tub} = \rho_b g Q/\Sigma$$

The barometric stiffness due to gravity forces, or the ratio between the pressure build-up at the well head and the expelled brine flow, in the case of a $\Sigma = 1$ m^2 container cross-section, is

$$\rho_b g/\Sigma = 10^{-2} \text{ MPa/m}^3$$

This stiffness is larger when the container cross-section is small (Figure 6). For example, if there is no container, and the air/brine interface is located inside the tube itself, the barometric stiffness due to gravity forces will be $\rho_b g/S = 40\ 10^{-2}$ MPa/m^3. In this case, the "upper string" would be much stiffer than the "lower string" constituted by the cavern.

A Very Large Harmonic Oscillator — The differential equation satisfied by flow-rate Q is simply reached by considering that brine in the tube, with mass $\mu = \rho_b SH$ and acceleration $a = \dot{Q}/S$, is pushed upward by the cavern pressure excess P_c (excess, when compared to static pressure distribution at rest) and pushed downward by the pressure excess at the bottom of the container P_{tub}, both pressures acting through the tube cross-section:

$$(\rho_b SH)(\ddot{Q}/S) = S(\dot{P}_c - \dot{P}_{tub})$$

Some straightforward algebra allows elimination of $\dot{P}_c$ and $\dot{P}_{tub}$:

$$\ddot{Q} + \left\{ \frac{S}{\rho_b H(\beta_c + \beta_b^{ad})V} + \frac{gS}{\Sigma H} \right\} Q = 0$$

The solution of such a differential equation is a sine function, whose period is

$$T = \frac{2\pi}{\omega_o} \quad , \quad \omega_o^2 = \frac{S}{\rho_b H(\beta_c + \beta_b^{ad})V} + \frac{gS}{\Sigma H}$$

• The test was performed in July 1982 on the Etrez 53 cavern. The cavern volume was $V \approx 7500$ m^3, the tube length, H, was 930 meters, and the tube cross-section, S, was 250 cm^2, the cavern was opened in a large container, Σ=several m^2, and the cavern compressibility was estimated to be $\beta V \approx 3$ m^3/MPa (see Figure 7). Data acquisition frequency was 7 Hz. At the beginning of the test, the main valve was closed and brine was forced into the cavern through a hydro-air pump to increase the cavern pressure. Then the main valve was opened (end of Phase 1) and a long period oscillation ($T = 74$ s) took place; this was measured through the pressure variations in the fuel-filled annular space. This figure was consistent with the computed value, which was $T \approx 73$ s. Figure 18 displays the results of a simulation (non-linear head losses have been taken into account).

2.4 Gas Pocket Trapped in the Well Head

The SPR3 cavern, with its abnormally high compressibility due to a gas pocket trapped in the cavern, has been described previously (paragraph 1.4.5). The well head was equipped with a pressure gauge whose resolution was 250 Pa; the data acquisition period was 0.05 s. The initial objective of the first test, called test 0, was to observe Helmholtz-resonator oscillations in the opened cavern, as had been made during the 1982 Etrez test. After build up of a small pressure excess in the closed cavern, opening of a well-head valve (which takes place 300 seconds after test start on Figure 8) vents the cavern and triggers short-period stationary quarter-waves, followed by a longer period oscillation. The period, assuming a tube cross-section $S = 81$ cm^2, should have been 145 seconds (see formula above); but dampening appear to be high (due to small tube cross-section) and the oscillation rapidly vanishes (Figure 8).

Much clearer, but totally unexpected, oscillations are triggered in the closed cavern when the injection pump stops, 100 seconds after test start. These oscillations are *anharmonic*: crests are spiky, and troughs are rounded, resulting in uncommon asymmetric pressure-versus-time curves. This effect dwindles, and the so-called "period" becomes smaller when signal amplitude is dampened with time. These facts are best shown on a further test in which initial amplitude was larger (Figure 9); the pressure origin is the same as in Figure 8. During a second series of tests (Figure 10), numbered from 1 to 7, 700 liters of brine were injected in 100-liter steps, again triggering anharmonic vibrations whose "periods" are significantly reduced (from 15 seconds to 8 seconds for the period measured just after pump stops) when the well head pressure increases following each brine injection. Only the existence of a very compressible non-linear elastic body included in the (cavern plus well) system can be responsible for these unexpected features. The gas pocket trapped in the cavern is not a good candidate — its high pressure (8.3 MPa) makes it a relatively stiff body. A better hypothesis appears to be the existence of a small amount of gas (a few liters) trapped at the well head in the annular space. Its pressure is close to atmospheric; then even small brine-gas interface displacements can drastically modify the gas volume and generate non-linear pressure build-up. If P and h are the gas-column (absolute) pressure and height, respectively, the adiabatic gas compression can be described as above:

$$P h^\gamma = P_1 h_1^\gamma$$

(Sub 1 refers to the figures when the cavern is at rest.) The cavern is compressible, as outlined above; displacement of the gas/brine interface from h_1 to h forces a volume, $\tilde{S}(h - h_1)$, into the cavern ($\tilde{S}$ is the annular cross-section area), that builds up the cavern pressure by

$$\beta V (P_c - P_c^1) = \tilde{S}(h - h_1)$$

Then the momentum equation for the brine column in the annular space can be written:

$$(H_a - h)(\rho_b \ddot{h} + \bar{\omega}) = P - P_1 - \rho_b g(h - h_1) - (P_c - P_c^1)$$

where H_a is the annular space length, and $\bar{\omega}$ are head losses (in Pa/m); typically, $\bar{\omega} = \kappa \ \mathrm{sgn}(\dot{h})^{1.85}$, where $\kappa = 1.35\ 10^6$ I.S. units. Some straightforward algebra leads to a non-linear differential equation that allows back-calculation of the gas column height (Figure 11): the best-fit sets the brine/gas interface 170 cm below the brine/air interface during test 0, which means that the gas pressure was $P_1 = 0.121$ MPa. After the test, the annular space was opened to the atmosphere and gas flew out of the well head.

Conclusions

Much useful information can be inferred from recording the pressure oscillations that are triggered when brine injection or withdrawal stops — for instance, the volume of a salt cavern, the LPG-volume/brine-volume ratio in a LPG storage cavern, and the existence of small gas pockets trapped in the well head. A further advantage is that information can be obtained for relatively *little cost*.

Acknowledgements: The authors have benefited from comments by Gerard Durup, of the Gaz de France Company, and Florian Lehner, visiting professor at Ecole Polytechnique. They are indebted to the staffs of the Etrez (GDF), Carresse (ELF), and Manosque (GEOSTOCK) storage sites, also to Yves Le Bras and Vincent De Greef from Ecole Polytechnique, who provided valuable assistance in performing the tests. Special thanks to Kathleen Sikora.

β	Compressibility Factor (C.F.)
β^{sat}	C.F. during a slow test
β_b	brine C.F.
β_b^{ad}	brine C.F. (rapid test)
β_c	cavern C.F.
β_{gas}^{isot}	gas C.F. (slow test)
β_h	hydrocarbon C.F.
β_{prop}	propane C.F.
γ	gas adiabatic constant
η	air-brine interface depth
κ	head-loss parameter
ν	Poisson's ratio
π	3.14
ρ_b	brine density
ρ_h	hydrocarbon density
$\delta\rho$	density gap
Σ	container cross section
ω_o	wave pulsation
$\bar{\omega}$	head losses per m of length
V	cavern volume
ΔV_{inj}	brine injected volume
V_{exp}	hydrocarbon expelled volume
x	hydrocarbon/cavern volume ration
a	acceleration
c	sound celerity (s.c.)
c_a	s.c. in air
c_b	s.c. in brine
c_f	s.c. in a fluid
c_w	s.c. in water
E	Young's modulus
f	shape factor
g	gravity acceleration
h	gas column length
h_1	gas column length at rest
h_i	saturated/unsaturated brine interface
H	central tube length
H_a	annular space length
H_i	hydrocarbon-brine interface depth
m	injected brine mass
M	cavern brine mass
P	fluid pressure
P_c	cavern pressure
P_{ann}	annular space well-head pressure
P_{tub}	central tubing well-head pressure
Q	brine flow rate
S	tube cross section
$\tilde{S}$	annular space cross section
T	period
u	brine flow speed

References

The SMRI papers referenced below are available through the Solution Mining Research Institute 1745 Chris Court - Deerfield, IL 60015-2079 USA.

1. Hardy R.H. and Langer M., *Proc. 1st Conf. Mech. Beh. Salt*, Trans Tech Pub., Clausthal-Zellerfeld, (1984) 901 pages.
2. Hardy R.H. and Langer M., *Proc. 2nd Conf. Mech. Beh. Salt*, Trans Tech Pub., Clausthal-Zellerfeld, (1988) 781 pages.
3. Hardy R.H., Langer M., Bérest P. and Ghoreychi M., *Proc. 3rd Conf. Mech. Beh. Salt*, Trans Tech Pub., Clausthal-Zellerfeld, (1996) 621 pages.
4. Aubertin M., Hardy R.H., *Proc. 4th Conf. Mech. Beh. Salt*, Trans Tech Pub., Clausthal-Zellerfeld, (1998) 658 pages.
5. Hugout B., "Mechanical behavior of salt cavities -in situ tests- model for calculating the cavity volume evolution". In *2nd Conf. Mech. Beh. Salt*, Trans. Tech. Pub., Clausthal-Zellerfeld, (1988) p. 291.
6. Ehgartner B.L. and Linn J.K., "Mechanical behavior of sealed SPR caverns", paper presented at the 1994 *S.M.R.I. Fall Meeting*, Houston.
7. Bérest P., Bergues J., Brouard B., Durup G. and Guerber B., "A tentative evaluation of the M.I.T.", paper presented at the 1996 *S.M.R.I. Spring Meeting*, Houston.
8. Boucly P., "In-situ tests and behaviour modelisation of salt cavities for storage of natural gas" (in French). *Rev. Fr. Géotechnique* (1982) **18**, p. 49.
9. Crotogino F.R., "Salt cavern in-situ testing from the constructor's and the operator's view point". *Proc. 1st Conf. Mech. Beh. of Salt*, Trans. Tech. Pub., Clausthal-Zellerfeld, (1984) p. 613.
10. Bérest P. and Brouard B., "Behavior of sealed solution-mined caverns". paper presented at the 1995 *S.M.R.I. Spring Meeting*, New-Orleans.
11. Clerc-Renaud A. and Dubois D., "Long term operation of underground storage in salt". *Proc. 5th Symp. on Salt*, Norther Ohio Geol. Soc., Cleveland, (1980), vol. II, p. 3.
12. Holzhausen G.R. and Gooch R.P., "The effect of hydraulic-fracture growth on free oscillations of wellbore pressure". *Proc. 26th U.S. Rock Mech. Symp.*, Rapid City, (1985) p. 621.
13. Bérest P., "Vibratory phenomena in oil drill holes. Application to the calculation of the volume of underground cavities" (in French), *Rev. Fr. Géotechnique* (1985), **32**, p. 5.
14. Hsu Y.C., "Forced oscillations of the Los Alamos Scientific Laboratory's Dry Hot Rock Geothermal Reservoir". *Report LA-6170-MS, Los Alamos Scientific Laboratories* (1975).
15. Bérest P., Habib P., Boucher M. and Pernette E., "Periodic flow of brine in the drilling hole of a salt cavern, Application to the determination of its volume". *Proc. 24th U.S. Rock Mech. Symp.*, (1983) p. 813.

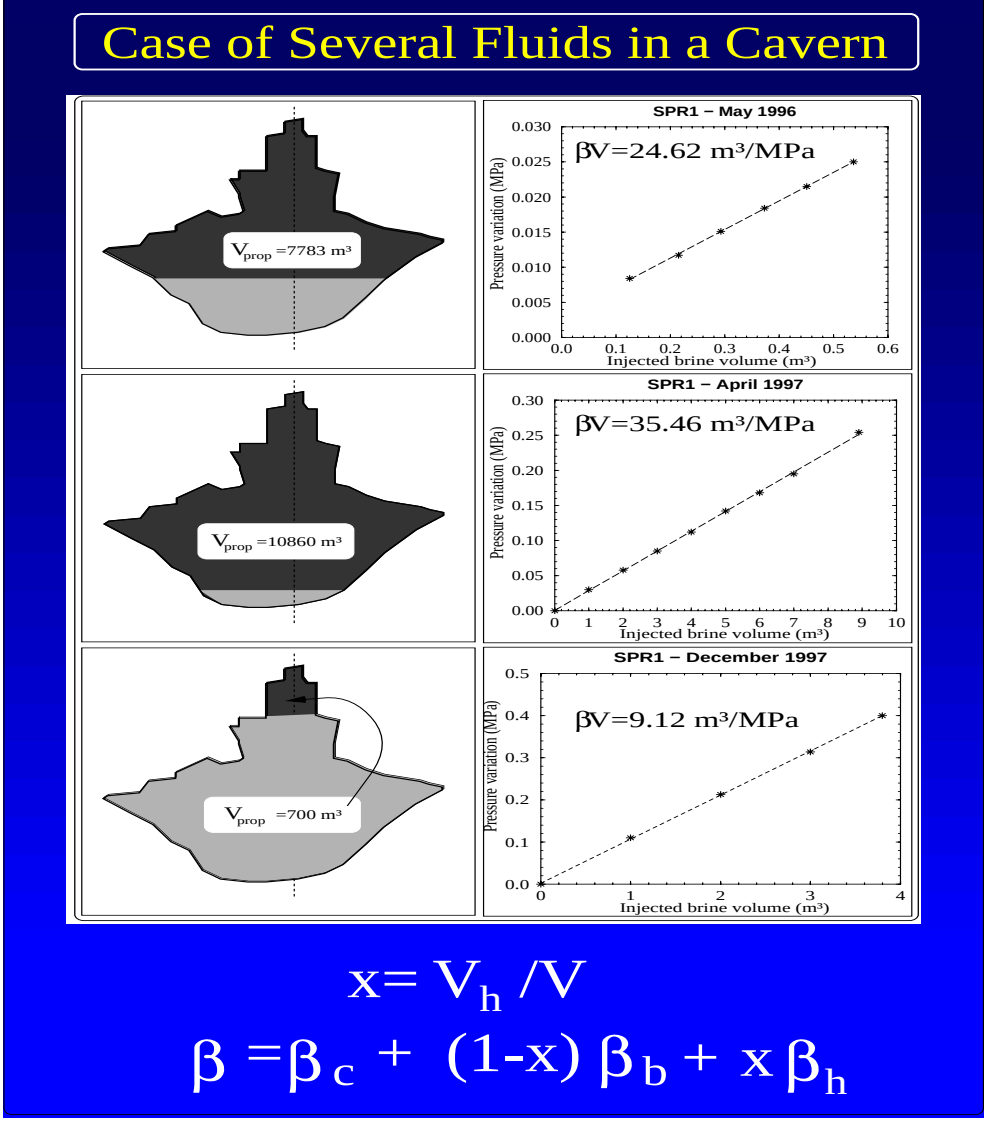

Figure 1: Three cavern compressibility measurements on the Carresse SPR1 cavern.

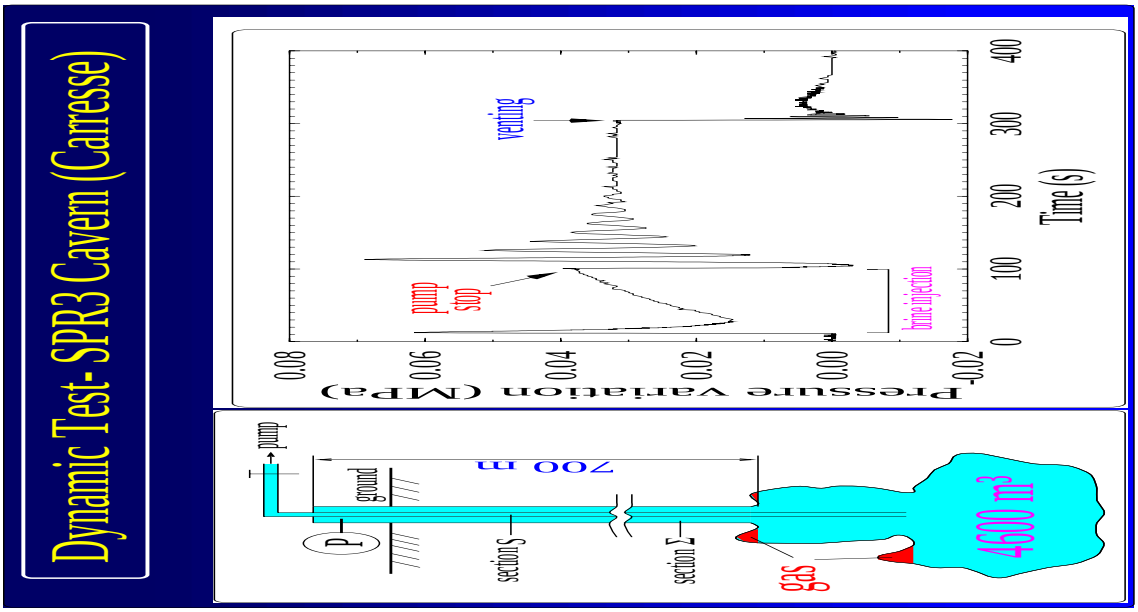

Figure 2: A compressibility test on the Carresse SPR3 cavern.

Figure 3: Blow-out movie.

Figure 4: Quarter-waves in the tubing during the July 1995 Carresse test (Elf Aquitaine).

Figure 5: The February 1995 Etrez test (Gaz de France).

Figure 6: A salt cavern considered as a mass and spring set.

Figure 7: The 1982 Etrez Test (Gaz de France).

Figure 8: The July 1995 test on SPR3 cavern (Elf Aquitaine).

Figure 9: Anharmonic oscillations during the July 1995 tests.

Figure 10: Pressure oscillations during brine injections.

Figure 11: Numerical simulation of anharmonic oscillations.